Electronic Supplementary Material (ESI) for Chemical Communications

A redox-active [3]rotaxane capable of binding and electrochemically sensing chloride and sulfate anions

Nicholas H. Evans, Christopher J. Serpell and Paul D. Beer

Supplementary Information

Table of Contents

Part I: Synthesis

General Information

Commerically available solvents and chemicals were used without further purification unless stated. Where dry solvents were used, they were degassed with nitrogen, dried by passing through a MBraun MPSP-800 column and then used immediately. Deionised water was used in all cases. Ferrocene was recrystallised from pentane. Triethylamine was distilled from and stored over potassium hydroxide. $(TBA)_2SO_4$ was prepared by concentrating a commercially available aqueous solution, then azeotroping the residue with dry THF with the resulting solid being dried and stored over P_2O_5 in a desiccator.

NMR spectra were recorded on Varian Mercury 300, Varian Unity Plus 500 and Bruker AVII 500 (with ^{13}C Cryoprobe) spectrometers. Mass spectra were carried out on Waters Micromass LCT, Waters GCT, Bruker micrOTOF and Bruker FT-ICR spectrometers. Melting points were recorded on a Gallenkamp capillary melting point apparatus and are uncorrected; where the sample decomposed before melting this is stated as Mp > xxx°C (dec.).

Experimental Procedure for Preparation of Axle $\mathbf{1}^{2+}(Cl^-)_2$

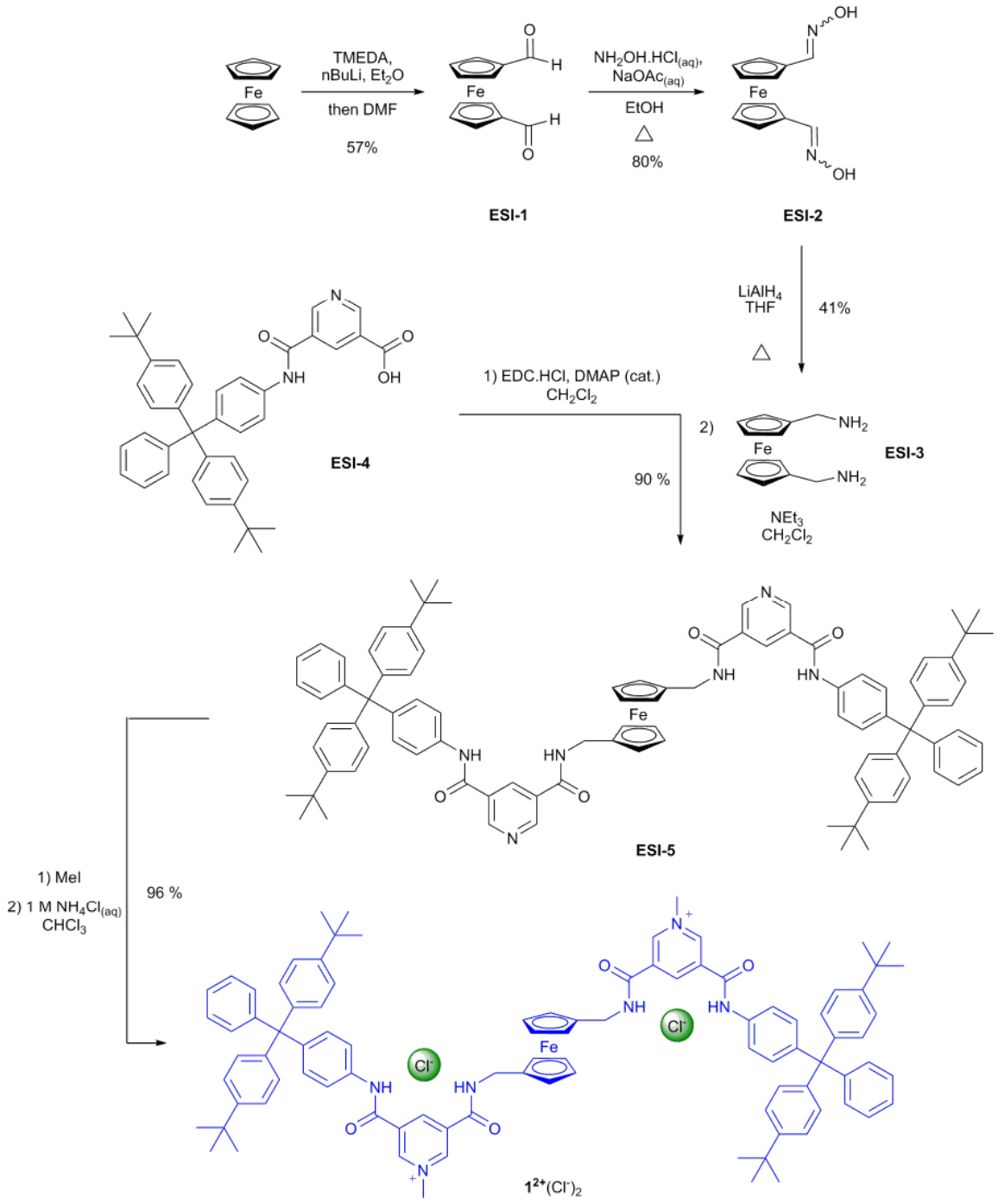

Supplementary Scheme 1: Preparation of axle $\mathbf{1}^{2+}(Cl^-)_2$

The preparation of 1,1'-diaminomethylferrocene **ESI-3** was by modification of literature procedures.[1,2] "Half-stoppered" pyridine **ESI-4**[3] and bisamine **2**[4] was prepared by published procedures.

Ferrocene-1,1'-dicarboxaldehyde **ESI-1**.[1]

To solution of TMEDA (3.12 g, 4.03 mL, 26.9 mmol) in dry Et_2O (30 mL) was added *n*BuLi in hexane (1.6 M soln, 16.8 mL, 26.9 mmol). This was stirred for 10 minutes, then ferrocene (2.00 g, 10.8 mmol) in dry Et_2O (60 mL) was added. The reaction mixture was stirred for 16 h, with a red precipitate being formed. The mixture was then cooled to -78 °C and dry, degassed, DMF (20 mL) added, and stirred at -78 °C for a further 2 h, with the precipitate being destroyed. After the reaction mixture warmed to room temperature, H_2O (100 mL) was added, and the aqueous layer extracted with EtOAc (4 × 200 mL). The combined organic layers were dried ($MgSO_4$), and the solvent removed, with the crude product being purified by silica gel column chromatography (EtOAc/Petrol 40°-60° 30:70 to 40:60) as a dark red solid (1.47 g, 57%). Mp = 156°C (dec.); δ_H (300 MHz, $CDCl_3$): 9.96 (2H, s, C*H*O), 4.89 (4H, app. s, Cp*H*), 4.68 (4H, app. s, Cp*H*); δ_C (75.5 MHz, $CDCl_3$): 192.8, 80.2, 74.2, 70.8; *m/z*: (ES) 243.0 ($[M + H]^+$, $C_{12}H_{11}FeO_2$ requires 243.0), 265.0 ($[M + Na]^+$, $C_{12}H_{10}FeNaO_2$ requires 265.0).

1,1'-Di(formyl)ferrocene oxime **ESI-2**.[2]

To a solution of ferrocene-1,1'-dicarboxaldehyde **SI 1** (0.62 g, 2.6 mmol) in EtOH (50 mL) at 50 °C was added an aqueous solution of $NH_2OH.HCl$ (0.71 g, 10 mmol in 5 mL of H_2O) and an aqueous solution of NaOAc (1.47 g, 17.9 mmol in 5 mL of H_2O). The reaction was stirred at 50 °C for 4 h and then almost all solvent was removed *in vacuo*. The residue was partitioned with Et_2O, separated, the organic layer dried ($MgSO_4$) and the solvent removed *in vacuo* to leave the product as a mixture of the three oxime isomeric products (0.56 g, 80%). δ_H (300 MHz, CD_3OD): 7.89 (s, 1H, N=C*H* arising from *E*, *Z* isomer), 7.87 (s, 2H, N=C*H* arising from *E*, *E* isomer), 7.13 (s, 1H, N=C*H* arising from *E*, *Z* isomer), 7.11 (s, 2H, N=C*H* arising from *Z*, *Z* isomer), 4.85 (t, ^3J = 1.9 Hz, 2H, Cp*H* arising from *E*, *Z* isomer), 4.80 (t, ^3J = 1.9 Hz, 4H, Cp*H* arising from *Z*, *Z* isomer), 4.56 (t, ^3J = 1.9 Hz, 4H, Cp*H* arising from *E*, *E* isomer), 4.52 (t, ^3J = 1.9 Hz, 2H, Cp*H* arising from *E*, *Z* isomer), 4.34-4.39 (m, 3 × 4H, Cp*H* arising from all 3 isomers); δ_H (300 MHz, d_6-DMSO): 11.05 (s, 1H, OH arising from *E*, *Z* isomer), 11.02 (s, 2H, OH arising from *Z*, *Z* isomer), 10.71 (s, 2H, OH arising from *E*, *E* isomer), 10.71 (s, 1H, OH arising from *E*, *Z* isomer). *m/z*: (ES) 295.0 ($[M + Na]^+$, $C_{12}H_{12}N_2NaO_2$ requires 295.0), 271.0 ($[M - H]^-$, $C_{12}H_{11}N_2O_2$ requires 271.0).

1,1'-Diaminomethylferrocene **ESI-3**.[2]

A suspension of $LiAlH_4$ (558 mg, 14.7 mmol) was refluxed under nitrogen in dry THF (15 mL) for 30 minutes. After cooling to room temperature, a solution of dioxime (200 mg, 0.735 mmol) in dry THF (15 mL) was added by dropping funnel over 10 minutes. The reaction mixture was refluxed under nitrogen for 16 h. The reaction mixture was cooled, a few drops of EtOAc added, then 10% NaOH (CAUTION!) until all inorganic salts precipitated out. The reaction mixture was filtered, washed with EtOAc and the filtrate was evaporated to dryness. The product was isolated as a yellow oily film after silica gel column chromatography (CH_3OH/NH_4OH 95:5) (73 mg, 41%). The product was used immediately in all cases. δ_H (300 MHz, $CDCl_3$): 4.15 (s, 2H, Cp*H*),

4.11 (s, 2H, Cp*H*), 3.58 (s, 4H, CH_2). *m/z*: (EI) 244.0663 ($[M^{\bullet}]^+$, $C_{12}H_{16}FeN_2$ requires 244.0663).

Dipyridyl **ESI-5**.

"Half-stoppered" pyridine **ESI-4**[3] (1.07 g, 1.79 mmol), EDC (377 mg, 1.97 mmol) and DMAP (cat.) were added to dry CH_2Cl_2 (20 mL) and stirred at 0°C under a N_2 atmosphere until all the solids dissolved. At this point, a solution of NEt_3 (199 mg, 0.27 mL, 1.97 mmol) and ferrocene diamine **ESI-3** (73 mg, 0.30 mmol) in dry CH_2Cl_2 (10 mL) was added at 0°C, and the reaction stirred for ~ 100 h under a N_2 atmosphere. The reaction mixture was washed with 10% citric acid (1 × 30 mL) and 10% $NaOH_{(aq)}$ (2 × 30 mL), the organic layer dried over $MgSO_4$, the solvent removed *in vacuo* and the crude material purified by silica gel chromatography (CH_2Cl_2/CH_3OH 97:3 to 96:4) to give the product as a yellow solid (375 mg, 90%). Mp > 180°C (dec.); δ_H (300 MHz, $CDCl_3$): 9.36 (2H, s, ArN*H*), 9.06 (2H, s, *ortho*-pyridinium Ar*H*), 9.02 (2H, s, *ortho*-pyridinium Ar*H*), 8.62 (2H, br s, *para*-pyridinium Ar*H*), 7.75 (2H, br s, CH_2NH), 7.47 (4H, d, ^3J = 8.8 Hz, stopper Ar*H*), 7.06-7.23 (30H, m, stopper Ar*H*), 4.27 (4H, d, ^3J = 5.3 Hz, CH_2NH), 4.08 (4H, s, Fc Cp*H*), 4.06 (4H, s, Fc Cp*H*), 1.28 (36H, s, $(CH_3)_3$); δ_C (75.5 MHz, $CDCl_3$): 165.1, 163.7, 151.1, 150.1, 148.4, 146.9, 144.1, 143.5, 135.3, 134.3, 131.7, 131.0, 130.8, 130.6, 129.5, 127.3, 125.7, 124.3, 119.5, 85.1, 68.8, 68.5, 63.7, 39.3, 34.3, 31.3; *m/z*: (ES) 1401.6597 ($[M + H]^+$, $C_{92}H_{93}FeN_6O_4$ requires 1407.6602).

Dichloride salt of axle $\mathbf{1}^{2+}(Cl^-)_2$.

A solution of dipyridyl **ESI-5** (365 mg, 0.260 mmol) in MeI (8 mL), was heated under reflux for 16 h. The excess MeI was removed *in vacuo* to give the dimethylated diiodide salt as a yellow solid. This was dissolved in $CHCl_3$ (75 mL) and washed with 1 M $NH_4Cl_{(aq)}$ (8 × 75 mL) and H_2O (2 × 75 mL). The organic layer was dried over $MgSO_4$ and the solvent removed *in vacuo* to give the chloride salt as a yellow-orange film (375 mg, 96%). Mp > 200°C (dec.); δ_H (300 MHz, $CDCl_3$): 10.95 (2H, s, ArN*H*), 10.26 (2H, s, *para*-pyridinium Ar*H*), 9.54 (2H, t, ^3J = 6.0 Hz, CH_2NH), 9.06 (2H, s, *ortho*-pyridinium Ar*H*), 8.10 (2H, s, *ortho*-pyridinium Ar*H*), 7.75 (2H, br s, CH_2NH), 7.95 (4H, d, ^3J = 8.8 Hz, stopper Ar*H*), 7.16-7.41 (30H, m, stopper Ar*H*), 4.30 (4H, d, ^3J = 6.0 Hz, CH_2NH), 4.21 (4H, s, Cp*H*), 4.15 (4H, s, Cp*H*), 3.85 (6H, s, N^+CH_3), 1.30 (36H, s, $(CH_3)_3$). δ_C (124.8 MHz, $CDCl_3$): 160.3, 158.3, 148.5, 147.5, 147.2, 145.6, 145.0, 143.7, 140.5, 135.2, 134.9, 134.1, 131.7, 131.0, 130.6, 127.6, 125.8, 124.5, 120.1, 86.5, 69.0, 67.7, 64.0, 49.1, 38.3, 34.3, 31.4; *m/z*: (ES) 1465.6698 ($[M - Cl]^+$, $C_{94}ClFeH_{98}N_6O_4$ requires 1465.6682).

Experimental Procedure for the Preparation of Rotaxane $\mathbf{3}^{2+}(Cl^-)_2$ *and* $\mathbf{3}^{2+}(PF_6^-)_2$

Dichloride salt of [3]rotaxane $\mathbf{3}^{2+}(Cl^-)_2$.

Axle $\mathbf{1}^{2+}(Cl^-)_2$ (245 mg, 0.165 mmol) and bis-amine $\mathbf{2}^4$ (153 mg, 0.320 mmol) were dissolved in dry CH_2Cl_2 (12 mL) and stirred for 30 minutes at 0°C under a N_2 atmosphere. NEt_3 (82 mg, 0.11 mL, 0.82 mol) was then added followed immediately by a dropwise addition of isophthaloyl dichloride (66 mg, 0.32 mmol) dissolved in dry CH_2Cl_2 (5 mL). The reaction was allowed to reach room temperature and stirred for 1 h. The reaction mixture was then washed with 10% citric acid (2 × 20 mL) and H_2O (1 × 20 mL), the organic layer dried ($MgSO_4$), the solvent removed *in vacuo* and the crude material purified by silica gel prep TLC (CH_2Cl_2/CH_3OH 97:3) to give the product as a yellow-orange solid (129 mg, 37%). Mp > 215°C (dec.); δ_H (300 MHz, $CDCl_3$): 10.07 (2H, s, pyridinium ArN*H*), 9.78 (2H, s, *para*-pyridinium Ar*H*), 9.11 (2H, t, ^3J = 5.9 Hz, pyridinium CH_2NH), 9.04 (2H, s, isophthalamide ArH^2), 8.95 (2H, s, *ortho*-pyridinium Ar*H*), 8.85 (2H, s, *ortho*-pyridinium Ar*H*), 8.66 (4H, br s, isophthalamide N*H*), 8.09 (4H, d, ^3J = 7.6 Hz, isophthalamide ArH^4 & ArH^6), 7.74 (4H, d, ^3J = 8.8 Hz, stopper Ar*H*), 6.98-7.34 (31H, m, isophthalamide ArH^5 & stopper Ar*H*), 6.27 (8H, d, ^3J = 8.8 Hz, hydroquinone Ar*H*), 6.05 (8H, d, ^3J = 8.8 Hz, hydroquinone Ar*H*), 4.63 (6H, s, N^+CH_3), 4.36 (4H, d, ^3J = 5.9 Hz, $CpCH_2NH$), 4.34 (4H, s, Cp*H*), 4.14-4.19 (4H, m, 0.5 × CH_2), 4.06 (8H, app s, Cp*H* & 0.5 × CH_2), 3.82-3.88 (4H, m, 0.5 × CH_2), 3.72-3.74 (36H, m, 4.5 × CH_2) 1.33 (36H, s, $(CH_3)_3$); δ_C (125.8 MHz, $CDCl_3$): 167.1, 159.3, 158.1, 153.7, 151.6, 148.4, 147.0, 145.0, 144.8, 144.4, 143.5, 134.7, 133.5, 133.5 (sic), 131.6, 131.6 (sic), 131.1, 130.6, 128.7, 127.3, 125.7, 124.9, 124.3, 120.3, 114.6, 114.5, 84.6, 70.7, 70.5, 70.0, 69.1, 68.3, 65.5, 63.8, 49.6, 41.1, 39.2, 34.3, 31.4; *m/z*: (ES) 1309.6065 ($[M - 2Cl]^{2+}$, $C_{158}H_{174}FeN_{10}O_{22}$ requires 1309.6071).

Dihexafluorophosphate salt of [3]rotaxane $\mathbf{3}^{2+}(PF_6^-)_2$.

A solution of $\mathbf{3}^{2+}(Cl^-)_2$ (95 mg, 0.035 mmol) dissolved in CH_2Cl_2 (15 mL) was washed with 0.1 M $NH_4PF_{6(aq)}$ (15 × 10 mL), then H_2O (5 × 10 mL). The organic layer was separated, dried over $MgSO_4$, and the solvent removed *in vacuo* to give the product as a yellow solid (89 mg, 86%). Mp = 168-170°C; δ_H (300 MHz, CD_3CN): 9.36 (2H, s, pyridinium ArN*H*), 8.96 (2H, s, *para*-pyridinium Ar*H*), 8.74 (4H, app s, *ortho*-pyridinium Ar*H*), 8.29 (2H, s, isophthalamide ArH^2), 8.01 (4H, d, ^3J = 9.4 Hz, isophthalamide ArH^4 & ArH^6), 7.93 (2H, br s, pyridinium CH_2NH), 7.55-7.60 (6H, m, isophthalamide ArH^5 & stopper Ar*H*), 7.15-7.39 (34H, m, isophthalamide N*H* & stopper Ar*H*), 6.55 (8H, d, ^3J = 9.1 Hz, hydroquinone Ar*H*), 6.27 (8H, d, ^3J = 8.8 Hz, hydroquinone Ar*H*), 4.35 (4H, d, ^3J = 5.3 Hz, $CpCH_2NH$), 4.28 (4H, s, Cp*H*), 4.16 (10H, app s, Cp*H* & N^+CH_3), 3.97-4.04 (8H, m, CH_2), 3.55-3.78 (40H, m, 5 x CH_2), 1.30 (36H, s, $(CH_3)_3$); δ_C (75.5 MHz, CD_3CN): 167.8, 160.6, 159.8, 153.9, 153.1, 149.8, 148.2, 147.0, 146.8, 145.7, 145.0, 136.0, 135.8, 134.8, 134.4, 132.3, 131.6, 131.5, 131.3, 130.1, 128.8, 127.0, 126.3, 125.7, 121.3, 116.4, 115.9, 85.0, 71.4, 71.3, 71.2, 70.7, 70.3, 68.7, 68.1, 64.9, 50.0, 40.7, 40.3, 35.0, 31.6; δ_F (282.4 MHz, CD_3CN): -72.9 (d, ^1J = 706 Hz, PF_6); δ_P (121.5 MHz, CD_3CN): -144.6 (septet, ^1J = 706 Hz, PF_6^-); *m/z*: (ES) 1309.6075 ($[M - 2PF_6]^{2+}$, $C_{158}H_{174}FeN_{10}O_{22}$ requires 1309.6071).

Dichloride salt of [2]rotaxane **ESI-6**$^{2+}$$(Cl^-)_2$

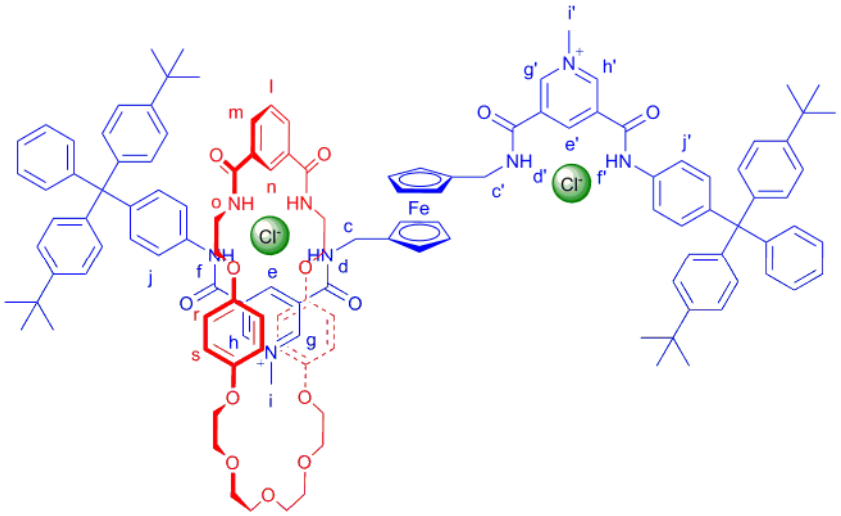

(only atoms assigned here and in spectra later are labelled)

This was isolated as a minor by-product from the reaction to form [3]rotaxane **3**$^{2+}$$(Cl^-)_2$ after further purification by silica gel prep TLC (CH_2Cl_2/CH_3OH 96:4) as a yellow-orange solid (isolated yield < 5 %). Mp > 200°C (dec.); δ_H (300 MHz, $CDCl_3$): 11.25 (1H, s, *f'*), 10.32 (1H, s, *e'*), 10.05 (1H, s, *f*), 9.79 (1H, br s., *d'*), 9.71 (1H, s, *e*), 9.34 (1H, s, *ortho*-pyridinium Ar*H*), 9.09 (1H, br s., *d*). 8.98 (3H, app s., *n* & 2 × *ortho*-pyridinium Ar*H*), 8.87 (1H, s, *ortho*-pyridinium Ar*H*), 8.64 (2H, br s., *o*), 8.05 (2H, d, ^3J = 8.8 Hz, *m*), 7.73-7.78 (4H, m, *j* & *j'*), 7.32 (1H, t, ^3J = 8.8 Hz, *l*), 7.00-7.27 (30H, m, stopper Ar*H*), 6.22 (4H, d, ^3J = 9.1 Hz, *r*), 6.03 (4H, d, ^3J = 9.1 Hz, *s*), 4.63 (3H, s, *i*), 4.36-4.38 (2H, m), 4.31 (app. 5H, app. s), 4.23 (app. 3H, app. s), 4.12 (2H, app. s), 4.05 (4H, app. s), 3.96 (2H, app. s), 3.69-3.79 (app. 21H, m), 1.32 (18H, s, $(CH_3)_3$), 1.30 (18H, s, $(CH_3)_3$); δ_C (125.8 MHz, $CDCl_3$): 167.2, 160.2, 159.4, 158.6, 158.1, 153.6, 151.6, 148.4, 147.2, 147.0, 146.5, 146.1, 145.0, 144.5, 144.4, 143.7, 143.5, 142.0, 135.4, 134.8, 133.5, 133.4, 131.6, 131.1, 130.6, 128.8, 127.4, 127.4 (sic), 125.7, 124.9, 124.4, 124.3, 120.2, 119.6, 114.6, 114.4, 85.1, 84.2, 70.6, 70.5, 70.1, 70.0, 69.4, 69.0, 68.7, 68.2, 65.4, 63.9, 63.8, 49.6, 49.0, 41.1, 39.4, 34.3, 31.4. (NB: many coincidental Ar*C*); *m/z*: (ES): 1012.9799 ($[M - 2Cl]^{2+}$, $C_{126}H_{136}FeN_8O_{13}$ requires 1012.9800).

The assignment of resonances between the multiplets δ: 3.69-3.79 & δ: 4.36-4.38 could not be accurately carried out, and so only apparent integration of the peaks is provided.

NB: [3]Rotaxane ***3***$^{2+}$$(Cl^-)_2$ *and, to a much greater extent, [2]rotaxane* ***ESI-6***$^{2+}$$(Cl^-)_2$ *were found to be slightly unstable on silica gel (reducing the yield in the case of the [2]rotaxane).*

Part II: Spectral Characterisation of Novel Compounds

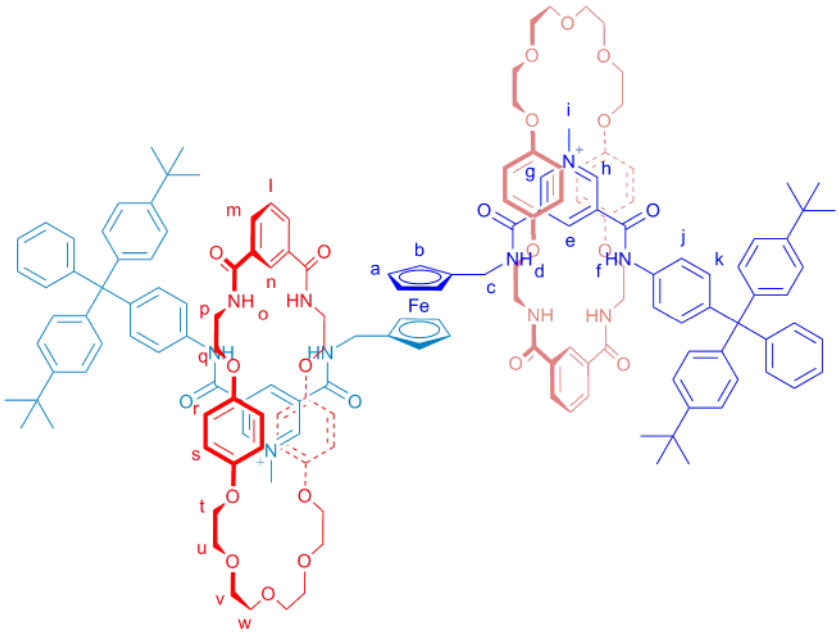

Supplementary Figure 1: Atom labels for [3]rotaxane $\mathbf{3}^{2+}(X^-)_2$ and its separated components

Dipyridyl **ESI-5**

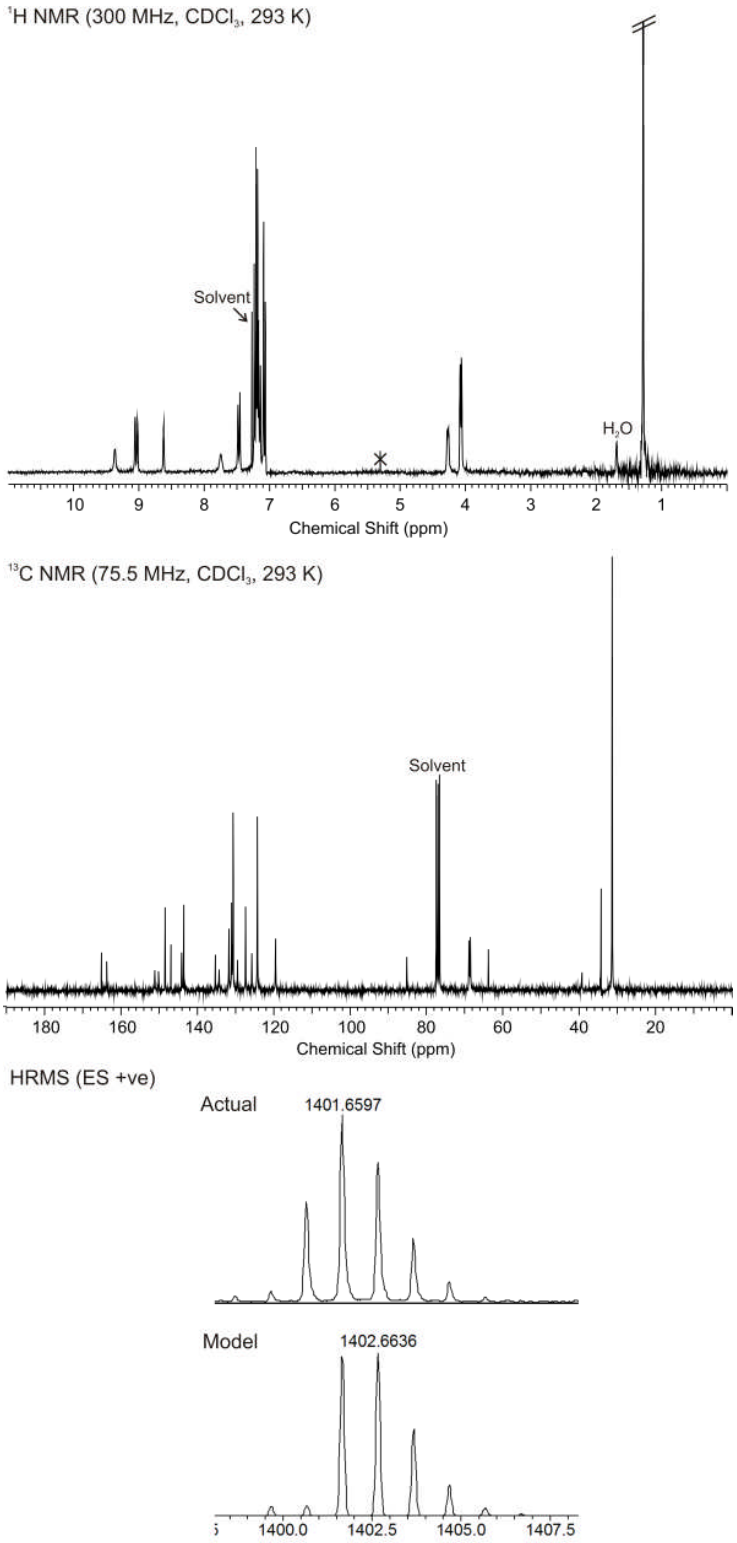

Supplementary Figure 2: ^{1}H and ^{13}C NMR and HR mass spectra of dipyridyl **ESI-5**.

Axle $\mathbf{1}^{2+}(Cl^-)_2$

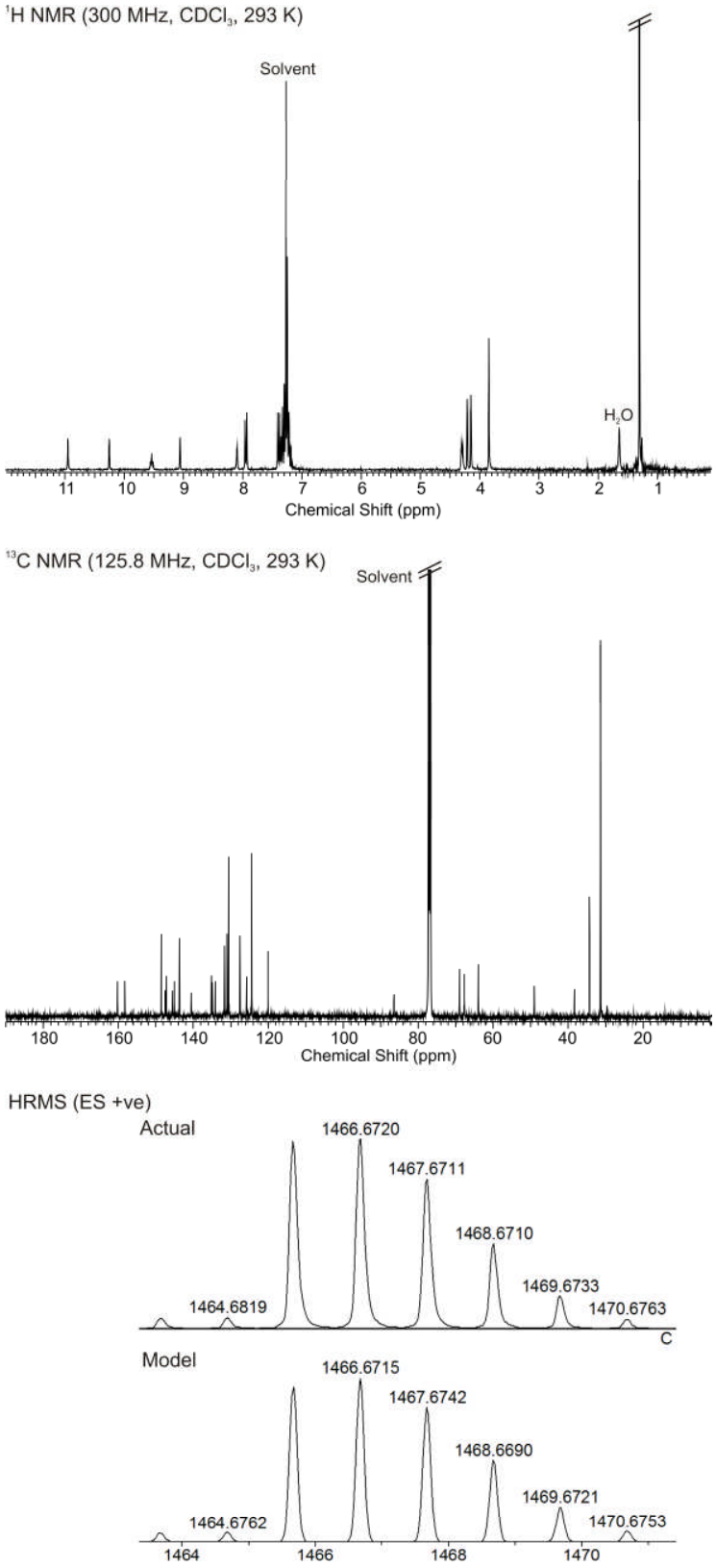

Supplementary Figure 3: ^{1}H and ^{13}C NMR and HR mass spectra of axle $\mathbf{1}^{2+}(Cl^-)_2$.

Axle $\mathbf{1}^{2+}(Cl^-)_2$ (cont.)

^{1}H COSY NMR (500 MHz, $CDCl_3$, 293 K)

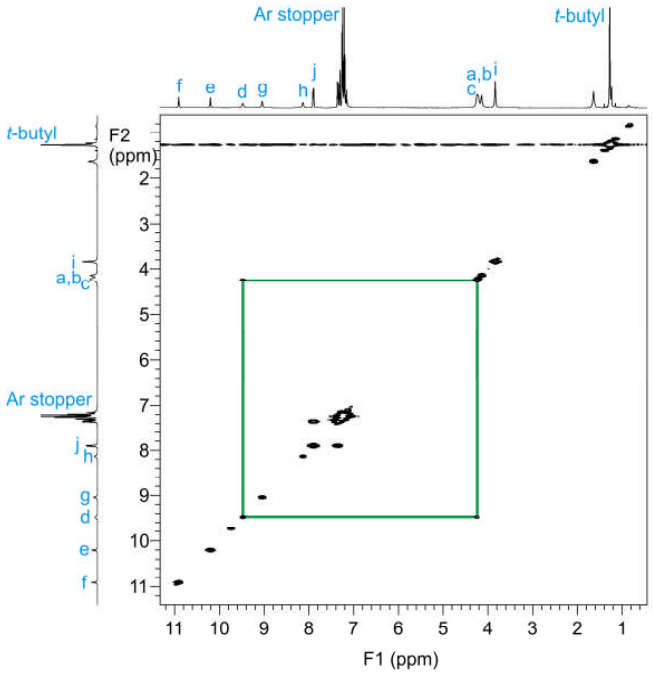

Diagnostic ^3J coupling of proton *c* to aliphatic amide *d* highlighted.

NB: Upon enhancement of spectrum ^4J couplings *e* - *g* and *e* - *h* are observed (not shown).

^{1}H ROESY NMR (500 MHz, $CDCl_3$, 293 K)

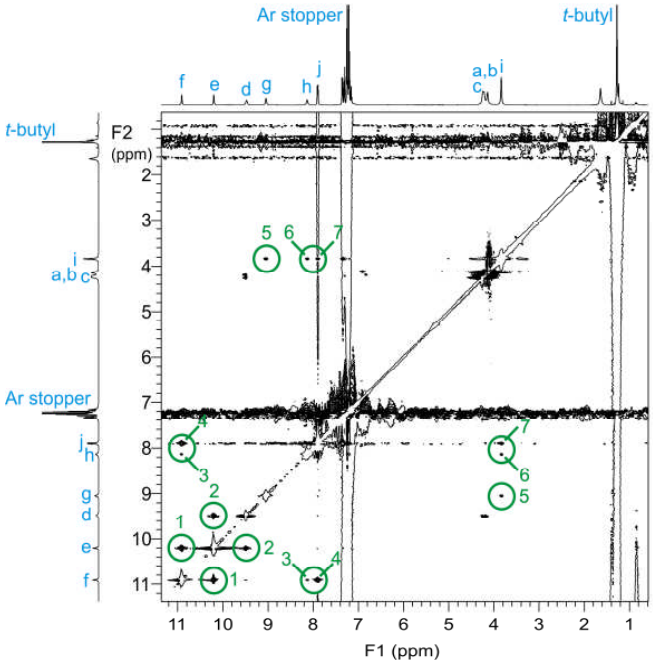

Diagnostic through space correlations highlighted.

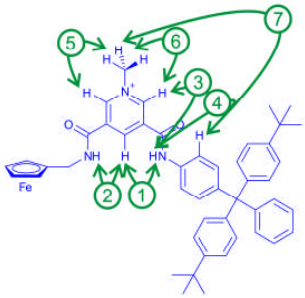

Supplementary Figure 4: ^{1}H COSY and ROESY NMR spectra of axle $\mathbf{1}^{2+}(Cl^-)_2$.

[3]Rotaxane $\mathbf{3}^{2+}(Cl^-)_2$

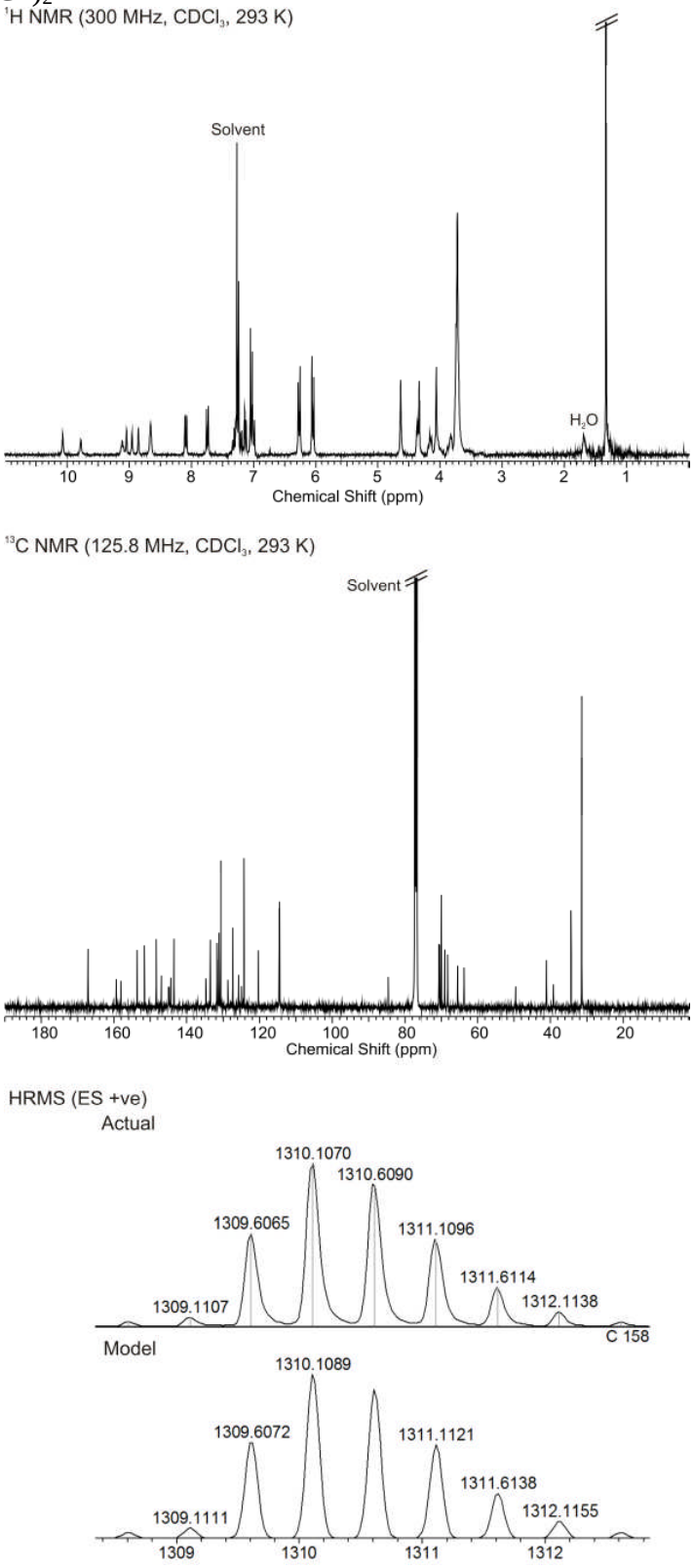

Supplementary Figure 5: ^{1}H and ^{13}C NMR and HR mass spectra of [3]rotaxane $\mathbf{3}^{2+}(Cl^-)_2$.

[3]Rotaxane $\mathbf{3}^{2+}(Cl^-)_2$ (cont.)

^{1}H COSY NMR (500 MHz, $CDCl_3$, 293K)

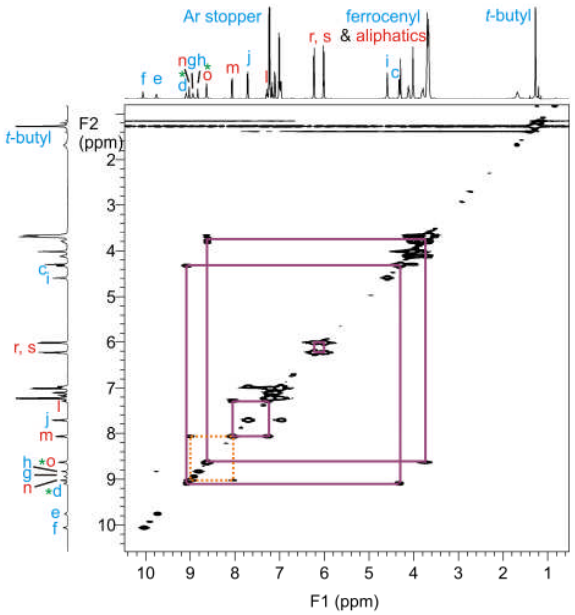

Aliphatic amides marked with asteriks.

^3J couplings marked with solid lines.

^4J couplings marked with dashed lines.

^{1}H ROESY NMR (500 MHz, $CDCl_3$, 293K)

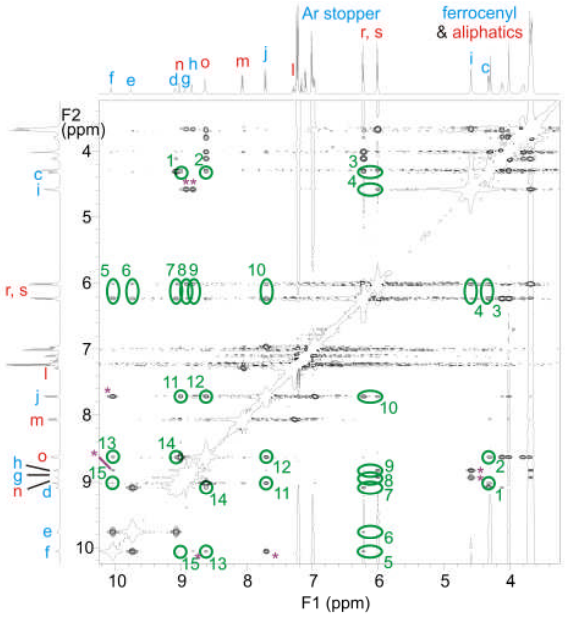

Principal unambiguously assignable through-space intercomponental interactions are circled.

Note: Intercomponental couplings are also observed between at least one set of ferrocenyl protons and the protons *n*, *o*, *r* and *s*.

Useful through-space intra-componental interactions are marked with an asterik. (in spectrum only)

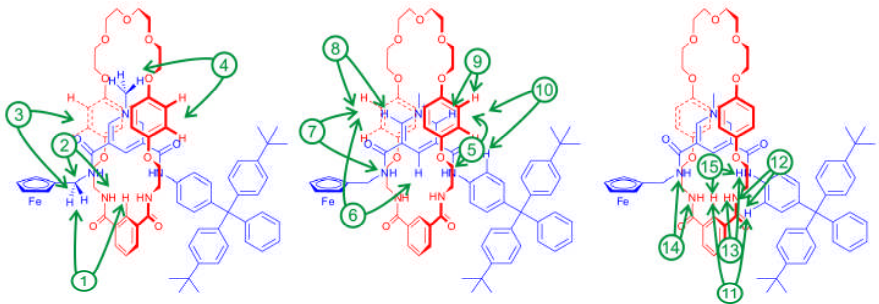

Supplementary Figure 6: ^{1}H COSY and ROESY NMR spectra (in $CDCl_3$) of [3]rotaxane $\mathbf{3}^{2+}(Cl^-)_2$.

[3]Rotaxane $\mathbf{3}^{2+}(Cl^-)_2$ (cont.)

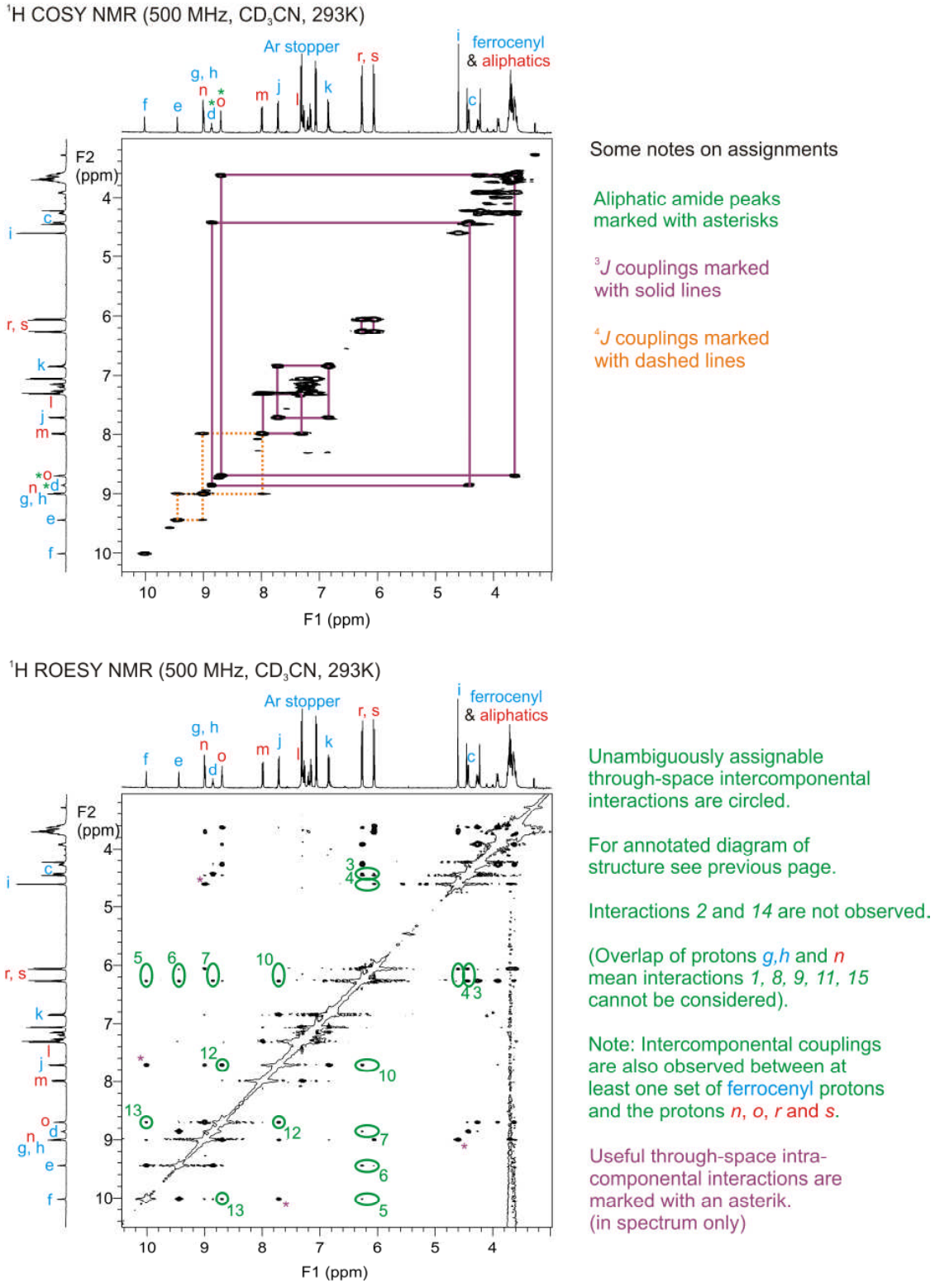

Supplementary Figure 7: ^{1}H COSY and ROESY NMR spectra (in CD_3CN) of [3]rotaxane $\mathbf{3}^{2+}(Cl^-)_2$.

[3]Rotaxane $\mathbf{3}^{2+}(PF_6^-)_2$

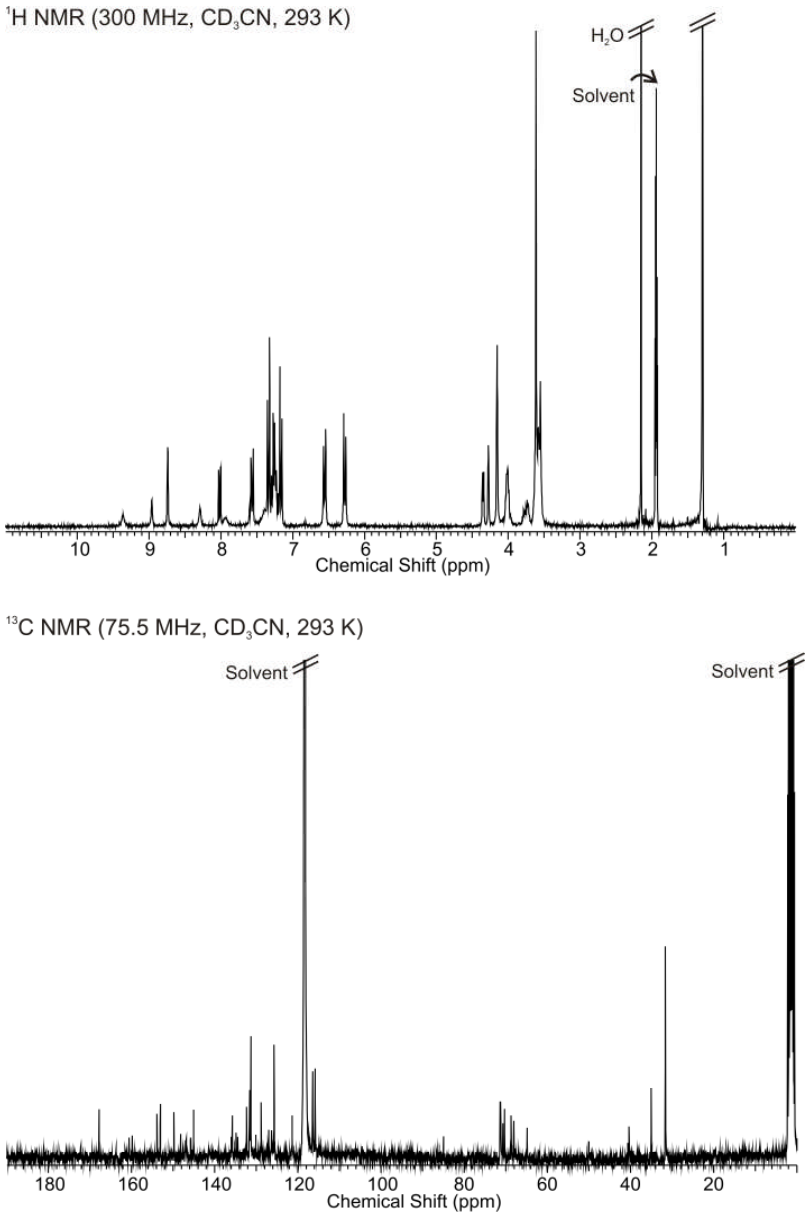

Supplementary Figure 8: ^{1}H and ^{13}C NMR spectra of [3]rotaxane $\mathbf{3}^{2+}(PF_6^-)_2$.

[3]Rotaxane $\mathbf{3}^{2+}(PF_6^-)_2$ (cont.)

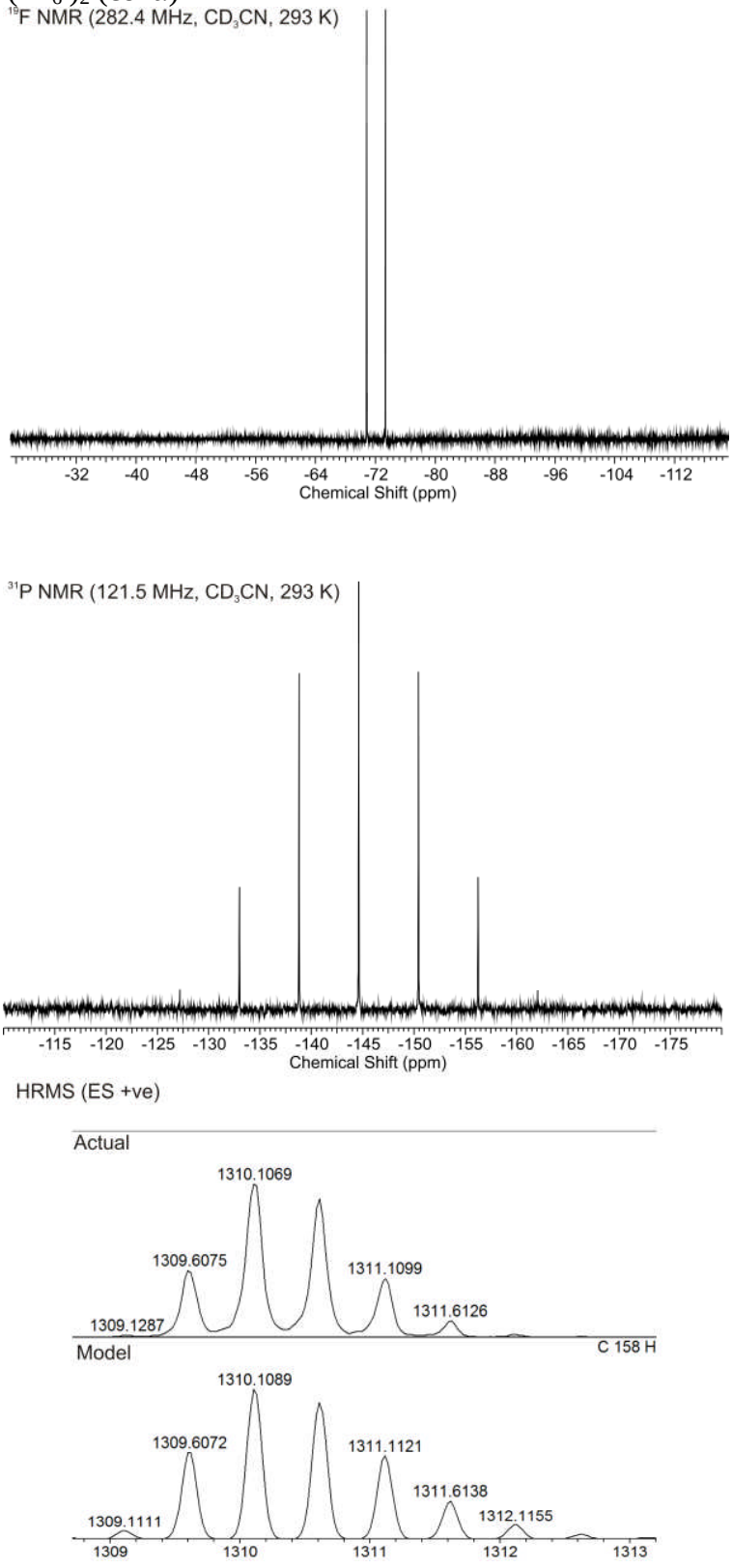

Supplementary Figure 9: ^{19}F and ^{31}P NMR and HR mass spectra of [3]rotaxane $\mathbf{3}^{2+}(PF_6^-)_2$.

[3]Rotaxane $\mathbf{3}^{2+}(PF_6^-)_2$ (cont.)

^{1}H COSY NMR (500 MHz, CD_3CN, 293K)

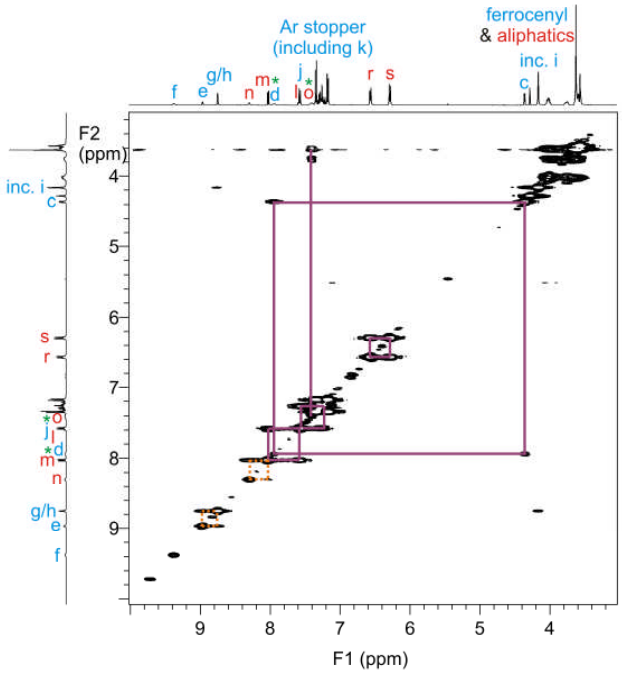

Some notes on assignments

Aliphatic amide peaks marked with asterisks

^3J couplings marked with solid lines

^4J couplings marked with dashed lines

^{1}H ROESY NMR (500 MHz, CD_3CN, 293K)

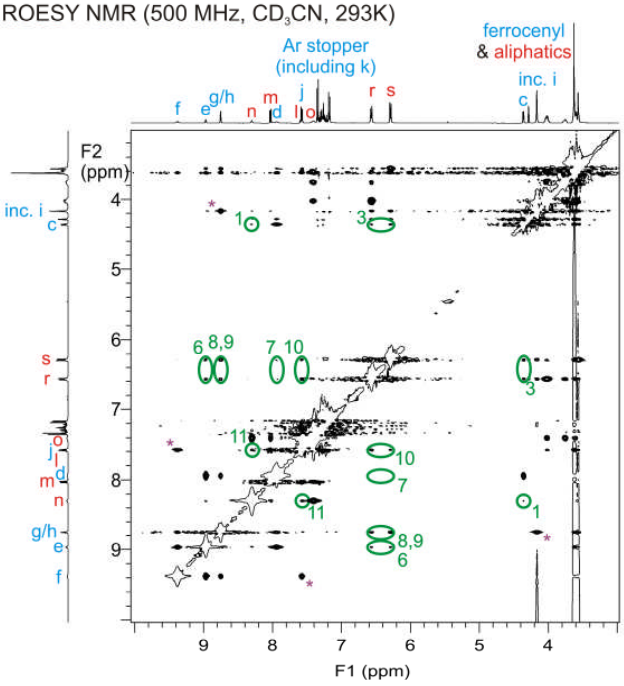

Unambiguously assignable through-space intercomponental interactions are circled.

For annotated diagram of structure see above.

Interactions *2*, *5*, *12*, *13*, *14* and *15* are not observed.

(Overlap of proton *l* means interaction *4* cannot be verified).

Note: Intercomponental couplings are also observed between at least one set of ferrocenyl protons and the protons *n*, *r* and *s*.

Useful through-space intra-componental interactions are marked with an asterik. (in spectrum only)

Supplementary Figure 10: ^{1}H COSY and ROESY NMR spectra of [3]rotaxane $\mathbf{3}^{2+}(PF_6^-)_2$.

[2]Rotaxane **ESI-6**$^{2+}$(Cl^-)$_2$

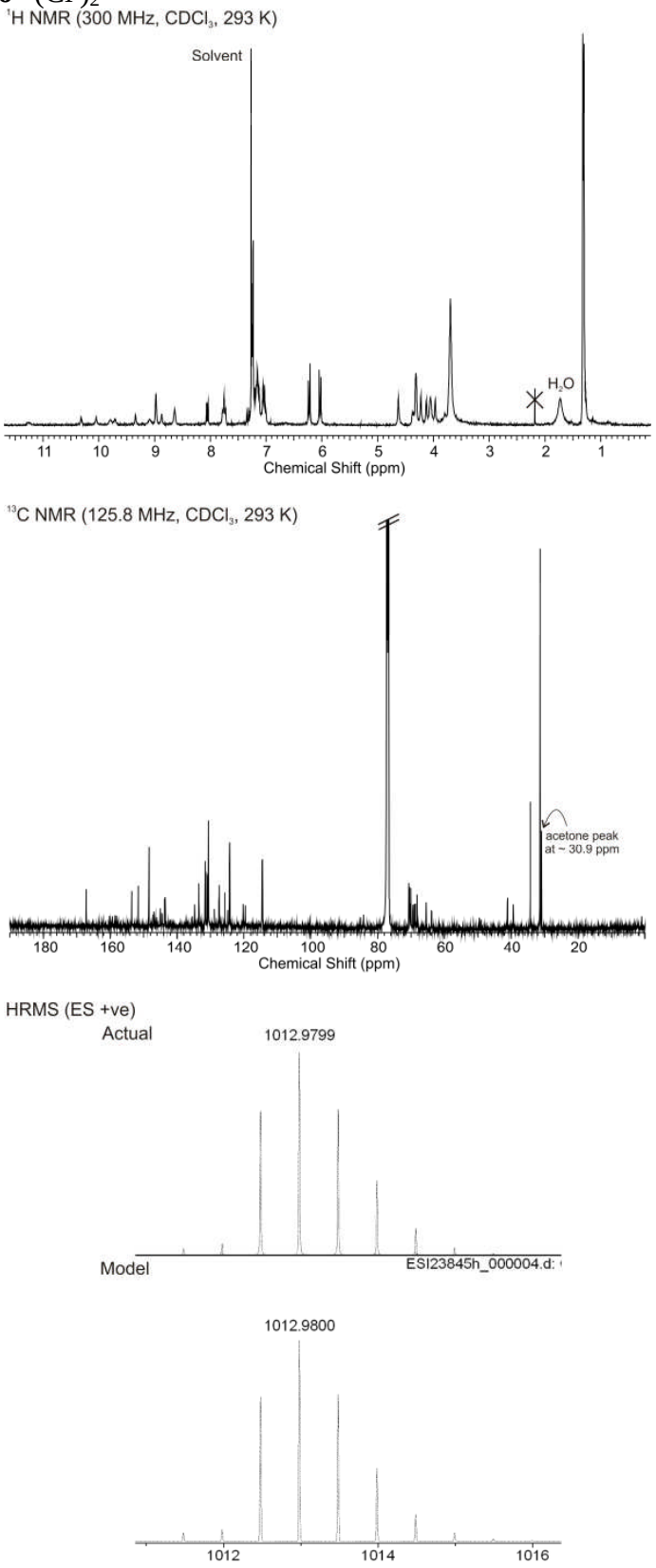

Supplementary Figure 11: ^{1}H and ^{13}C NMR and HR mass spectra of [2]rotaxane **ESI-6**$^{2+}$(Cl^-)$_2$.

[2]Rotaxane **ESI-6**$^{2+}$$(Cl^-)_2$ (cont.)

^{1}H COSY NMR (500 MHz, $CDCl_3$, 293 K)

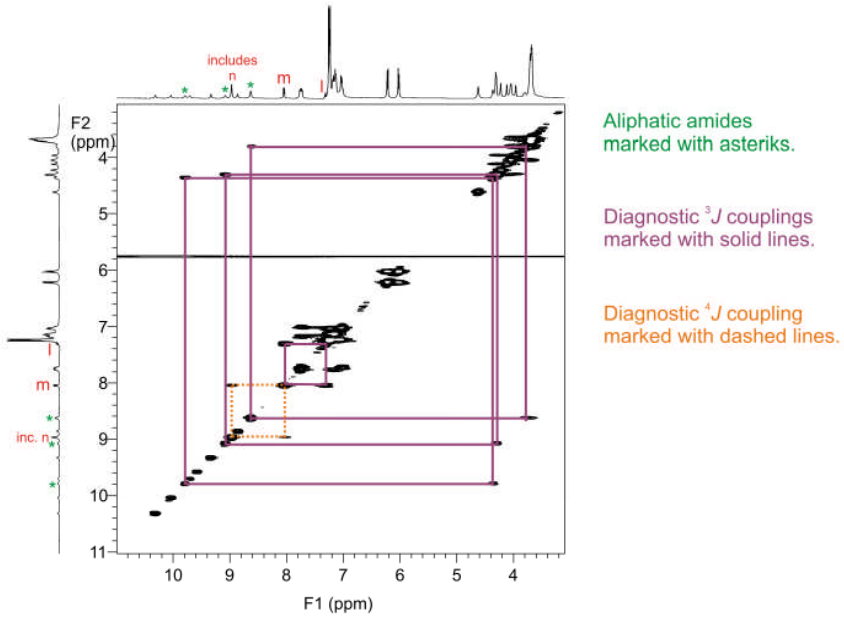

^{1}H ROESY NMR (500 MHz, $CDCl_3$, 293 K)

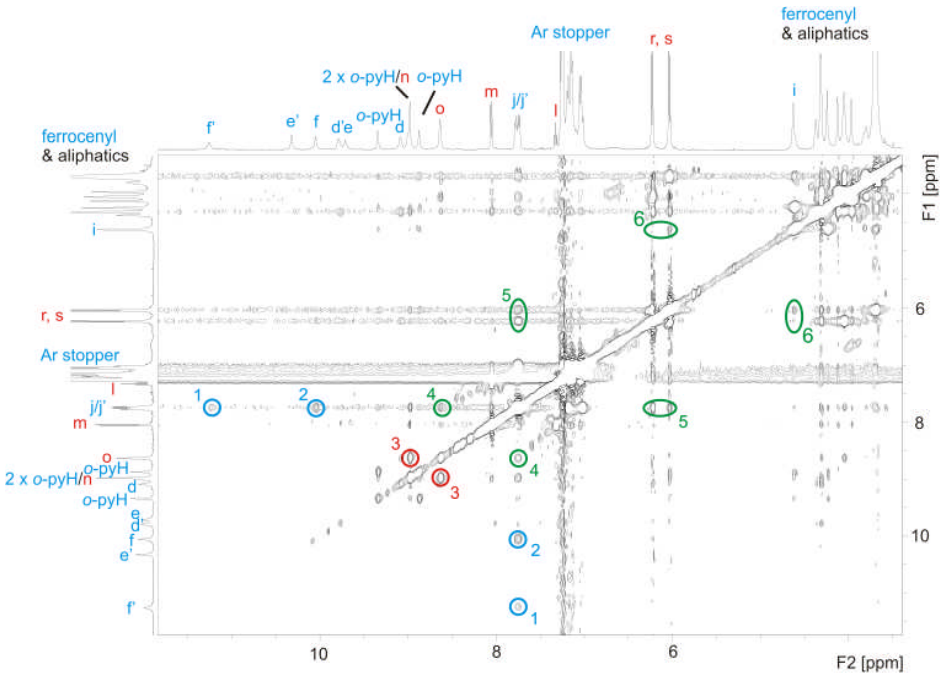

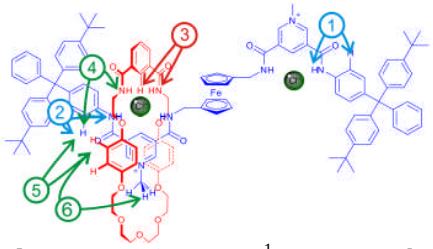

Useful intracomponental couplings are highlighted in blue and red.

Unambiguous intercomponental couplings are highlighted in green.

The full assignment of the *ortho*-pyridinium protons *g*, *h*, *g'* and *h'* is not given due to ambiguity between this 2D NMR spectrum and the comparison of the 1D ^{1}H NMR spectra of the axle and [3]rotaxane.

Supplementary Figure 12: ^{1}H COSY and ROESY NMR spectra of [2]rotaxane **ESI-6**$^{2+}$$(Cl^-)_2$.

Additional Spectral Comparisons of [3]Rotaxanes $\mathbf{3}^{2+}(Cl^-)_2$ and $\mathbf{3}^{2+}(PF_6^-)_2$

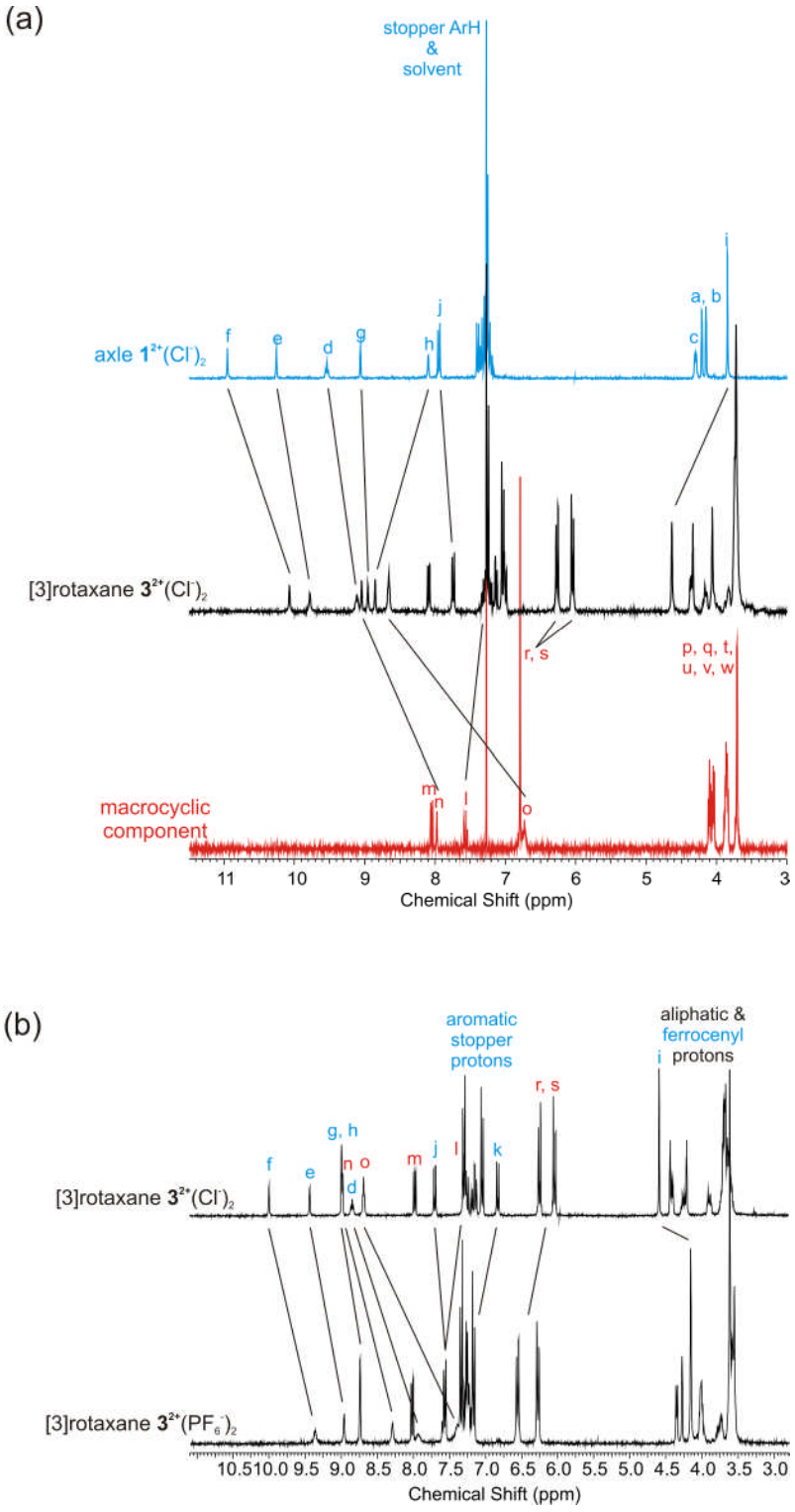

Supplementary Figure 13: (a) Partial ^{1}H NMR spectra of axle $\mathbf{1}^{2+}(Cl^-)_2$, [3]rotaxane $\mathbf{3}^{2+}(Cl^-)_2$ and free macrocyclic component (Solvent: $CDCl_3$, T = 293 K) and (b) Partial ^{1}H NMR spectra of [3]rotaxane $\mathbf{6}^{2+}(Cl^-)_2$ and [3]rotaxane $\mathbf{6}^{2+}(PF_6^-)_2$ (Solvent: CD_3CN, T = 293 K). For atom labels see diagram above.

Part III: Crystallographic Data

Crystallographic Data for [3]Rotaxane $\mathbf{3}^{2+}(Cl^-)_2$.[5]

Crystals were grown by slow diffusion of diisopropyl ether into a chloroform solution of $\mathbf{3}^{2+}(Cl^-)_2$. Single crystal X-ray diffraction data were collected using silicon double crystal monochromated synchrotron radiation (λ = 0.68890 Å) at Diamond Light Source beamline I19 using a custom-built Rigaku diffractometer equipped with a Cryostream N_2 open-flow cooling device.[6] The data were collected at 150(2) K via a series of ω-scans were performed in such a way as to cover a sphere of data to a maximum resolution of 0.77 Å. Cell parameters and intensity data (including inter-frame scaling) were processed using the CrystalClear package.[7] The structure was solved by charge flipping using Superflip[8] and refined against full matrix F^2 within the CRYSTALS suite.[9]

Some disorder was identified in the *tert*-butyl groups, and more significantly in the chloroform molecules close to the main residue which could be discerned from the diffraction data. Refined partial occupancies were used to model these portions. Although a few isolated points of electron density could be discerned in the larger void, no sensible solvent structure model could be constructed and so PLATON SQUEEZE[10] was used to include this volume of diffuse electron density in the refinement. Geometric restraints were applied to the solvent molecules and vibrational restraints to the whole structure. After pruning the Wilson plot to eliminate absent high angle data, the locations of the non-disordered hydrogen atoms could be seen in the Fourier difference map. These were located geometrically and refined against the data using restraints, after which their positions were constrained using rides.

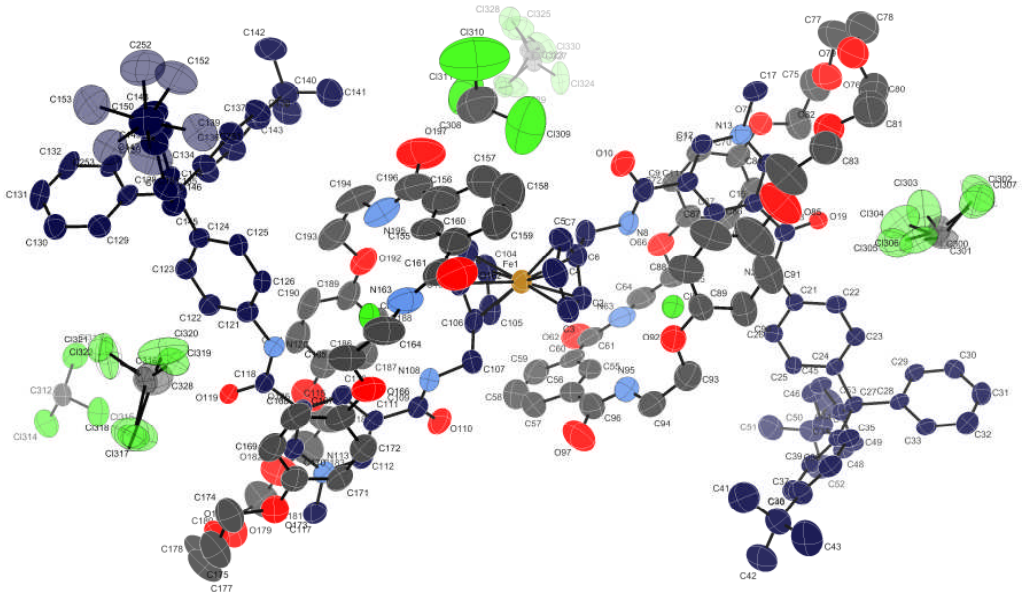

Supplementary Figure 14: X-ray crystal structure of [3]rotaxane $\mathbf{3}^{2+}(Cl^-)_2$. Thermal ellipsoids set at 50 % probability.

Supplementary Table 1: Selected crystallographic data for [3]rotaxane $\mathbf{3}^{2+}(Cl^-)_2$

Compound reference	$\mathbf{3}^{2+}(Cl^-)_2$
Chemical formula	$C_{163}H_{177}Cl_{17}Fe_1N_{10}O_{22}$
Formula Mass	3286.81
Crystal system	Triclinic
a/Å	16.141(11)
b/Å	21.623(15)
c/Å	24.192(17)
α/°	96.343(14)
β/°	93.555(17)
γ/°	97.116(4)
Unit cell volume/Å^3	8300(10)
Temperature/K	150
Space group	$P\bar{1}$
No. of formula units per unit cell, *Z*	2
No. of reflections measured	34946
No. of independent reflections	34946
R_{int}	0.119
Final R_1 values ($I > 2\sigma(I)$)	0.1391
Final $wR(F^2)$ values ($I > 2\sigma(I)$)	0.2982
Final R_1 values (all data)	0.1720
Final $wR(F^2)$ values (all data)	0.3271

Part IV: Anion Recognition Studies

^{1}H NMR Titrations

Protocol

^{1}H NMR spectra were recorded on a Varian Unity Plus 500 spectrometer. In a typical experiment, a solution of guest was added to a solution of the host at 293 K. The chemical shift of specific proton(s) was monitored for seventeen titration points (for 0, 0.2, 0.4, 0.6, 0.8, 1.0, 1.2, 1.4, 1.6, 1.8, 2.0, 2.5, 3.0, 4.0, 5.0, 7.0 and 10.0 equivalents of added guest), with the resulting data analysed using the WinEqNMR2 computer program,[11] as the association of guest and host was found to be fast on the NMR timescale for all systems.

The anion binding titration experiments were carried out using salts of the non-complexing tetrabutylammonium (TBA) cation as the guest species, titrated into the dissolved host. A 0.075 M solution of anion was added to 0.50 mL of a 1.50 mM solution of host, i.e. 10 μL is 1 equivalent. The volumes of TBA salt added were 10 x 2 μL, 2 x 5 μL, 2 x 10 μL, 1 x 20 μL and 1 x 30 μL.

The values of the observed chemical shift and the guest concentration were entered into winEQNMR2 for every titration point and, estimates for the binding constant and limiting chemical shifts were made. The parameters were refined using non-linear squares analysis to obtain the best fit between observed and calculated chemical shifts for either a 1:1 or 2:1 (guest to host) binding stoichiometry. The program plots the observed chemical shift versus the guest concentration, revealing the accuracy of the experimental data and the suitability of the model used. The input parameters were varied until the best-fit values of the stability constants, and their errors, converged. The errors of the experimental data fitting to calculated binding isotherm were calculated to be < 15%.

Electrochemical Titrations

Protocol

Cyclic voltammetry (CV) and square wave voltammetry (SWV) were performed on an Autolab Potentiostat/Galvanostat model PG-STAT 12, controlled by General Purpose Electrochemical System Software v. 4.9 (Eco Chemie). A standard one-compartment three-electrode electrochemical cell, located inside a Faraday cage, was used with a glassy carbon solid disc working electrode, a platinum wire auxiliary electrode and an Innovative Instruments, Inc. LF-2 leak-free silver/silver chloride reference electrode. A 0.5 mM ferrocene sample was used to check the reference electrode and internal resistance of the equipment. The electrolyte solution used in all experiments was 0.1 M $TBAPF_6$ in CH_3CN.

CVs were typically recorded with a 1 s equilibration time, a step potential of 1 mV and a scan rate of 100 mVs^{-1}. SWVs were typically recorded with a 1 s equilibration time, a step potential of 3 mV and a frequency of 30 Hz. The working electrode was cleaned between scans by polishing with commercially available microcloth.

In a typical experiment, the host (0.5 mM) was dissolved in 2.5 mL of a solution of $TBAPF_6$ (0.1 M) and cyclic and square wave voltammograms were recorded. For the cyclic voltammetry scan rates of 25, 50, 75, 100, 250 and 500 mVs^{-1} were used to test for reversibility. Anion binding experiments were performed by addition of 0, 0.5, 1, 1.5, 2, 3 and 5 equivalents of anion (as a 0.25 M solution of TBAX salt in electrolyte solution, 5 µL is 1 equivalent) to a 2.5 mL aliquot of the receptor solution, stirred and the cyclic and square wave voltammograms recorded.

Additional Data

I. Reversibility

For an electrochemical system (under fast kinetics) to be described as reversible, the following criteria must be satisfied:

(i) ΔE = 59/n mV (where n = number of electrons transferred in the redox process), so here where n = 1, ΔE should equal 59 mV;
(ii) E_{pa} and E_{pc} are independent of the scan rate;
(iii) $I_{pa} / I_{pc} = 1$;
(iv) I_{pa} and I_{pc} are proportional to the square root of the scan rate.

From CVs of [3]rotaxane $\mathbf{3}^{2+}(PF_6^-)_2$ recorded at varying scan rates, it is best to describe rotaxane $\mathbf{3}^{2+}(PF_6^-)_2$ as being quasi-reversible electrochemical systems.

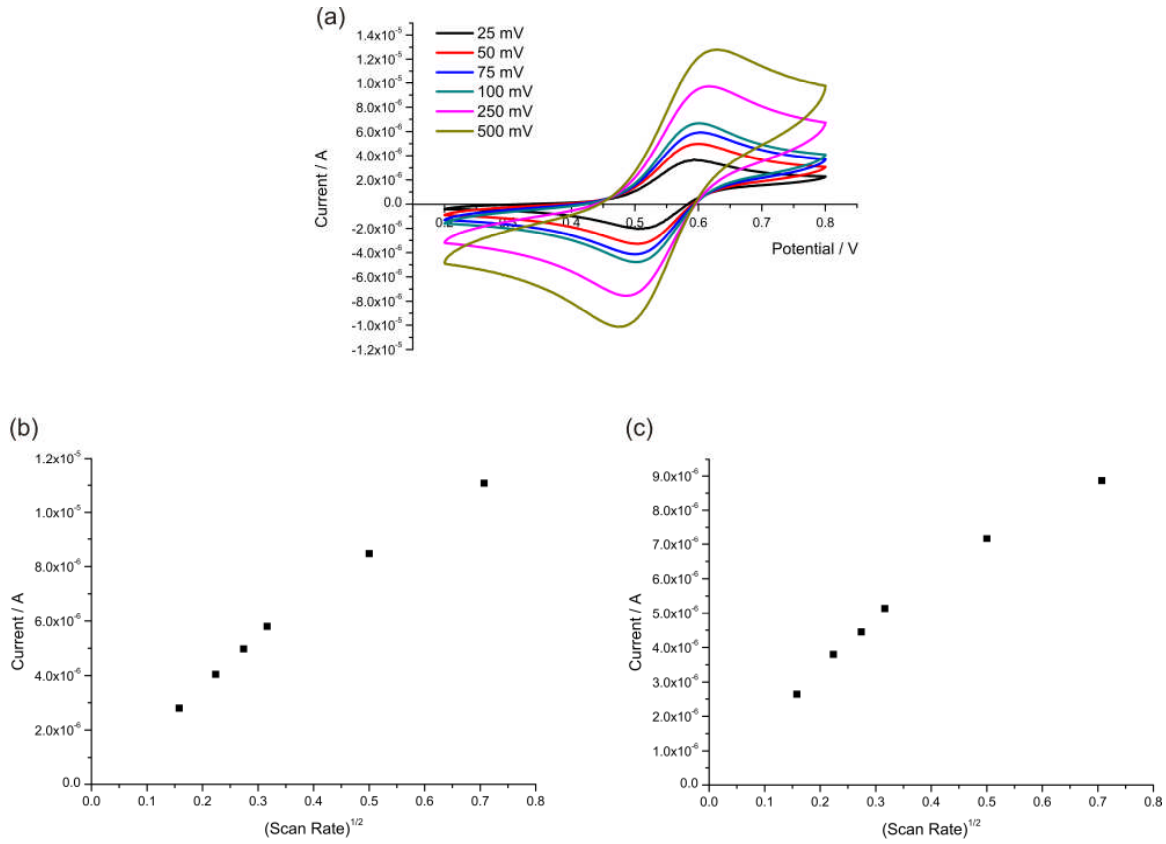

Supplementary Figure 15: (a) CVs of [3]rotaxane $\mathbf{3}^{2+}(PF_6^-)_2$ at various scan rates, (b) plot of I_{pa} vs (scan rate)$^{1/2}$ and (c) plot of I_{pc} vs (scan rate)$^{1/2}$. (Electrolyte: 0.1 M $TBAPF_6/CH_3CN$. Potential compared to a Ag/AgCl reference)

Scan Rate / mV	ΔE / V	E_{pa} / V	E_{pc} / V	I_{pa}/I_{pc}
25	0.079	0.593	0.514	1.06
50	0.080	0.592	0.512	1.07
75	0.092	0.600	0.508	1.12
100	0.087	0.597	0.510	1.13
250	0.111	0.610	0.499	1.18
500	0.130	0.622	0.492	1.25

Supplementary Table 2: ΔE, E_{pa}, E_{pc} and I_{pa}/I_{pc} data for [3]rotaxane $\mathbf{3}^{2+}(PF_6^-)_2$ for various scan rates. (Electrolyte: 0.1 M $TBAPF_6/CH_3CN$. Potential compared to a Ag/AgCl reference)

II CVs of sulfate anion titration experiment

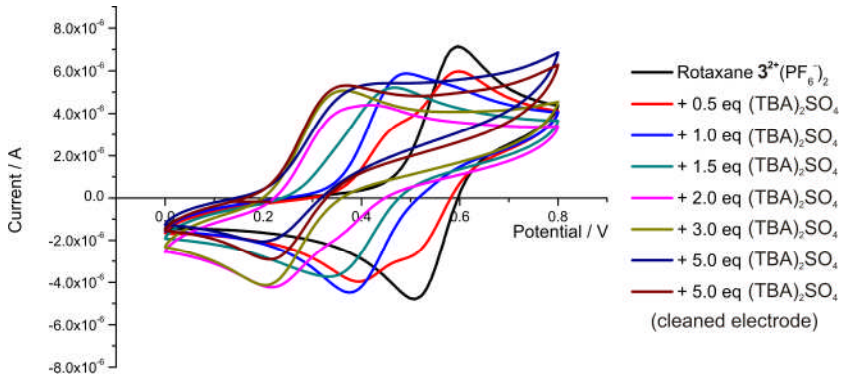

Supplementary Figure 16: CVs of [3]rotaxane $\mathbf{3}^{2+}(PF_6^-)_2$ upon the addition of $(TBA)_2SO_4$. (Electrolyte: 0.1 M $TBAPF_6/CH_3CN$. Potential compared to a Ag/AgCl reference)

At 0.5 equivalents of added anion, two-wave, slow kinetic electrochemical behaviour is observed. From 1 to 5 equivalents of added anion, a pseudo-single wave is observed to move cathodically but with a very wide peak separation (up to 200 mV). Close inspection of the SWV (see below) suggests some re-appearance of two-wave behaviour at 2 equivalents of added anion. A maximum cathodic shift $\Delta E_{1/2}$ = - 265 mV at 5 equivalents of added anion.

The electrodes were cleaned at the end of the titration to check whether precipitation was occurring on the electrode surfaces. However, relatively little change in the values of E_{pa} and E_{pc} was observed suggesting the large values of $\Delta E = (E_{pa} - E_{pc})$ observed are due to the intrinsic properties of the system being investigated.

An attempt to investigate the binding of sulfate by [3]rotaxane $\mathbf{3}^{2+}(PF_6^-)_2$ in CD_3CN by ^1H NMR titration experiment were thwarted by precipitation of the rotaxane-sulfate complex at sub-stoichemitric amounts of anion. Such precipitation probably does not occur in the electrochemistry experiment due to the presence of $TBAPF_6$ in the background electrolyte.

III. SWVs of anion titration experiments

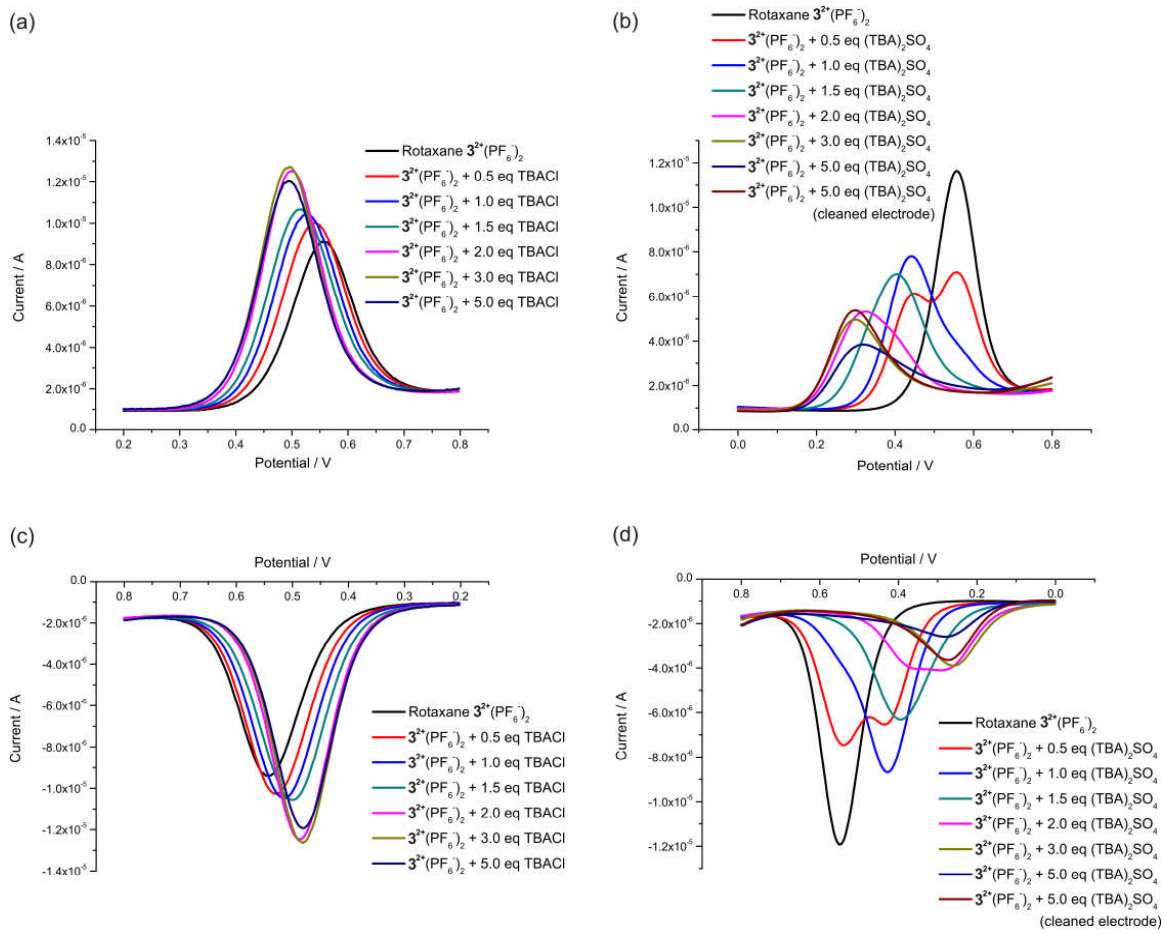

Supplementary Figure 17: SWVs of [3]rotaxane $\mathbf{3}^{2+}(PF_6^-)_2$ upon the addition of (a) & (c) TBACl and (b) & (d) $(TBA)_2SO_4$. (Electrolyte: 0.1 M $TBAPF_6/CH_3CN$. Potential compared to a Ag/AgCl reference, $E_{1/2}$ of [3]rotaxane $\mathbf{3}^{2+}(PF_6^-)_2$ = + 125 mV compared to $E_{1/2(ferrocene)}$ = 0 V.)

Part V: References

1. M. A. Carroll, D. A. Widdowson and D. J. Williams, *Synlett*, 1994, 1025.
2. F. Ossola, P. Tomasin, F. Benetollo, E. Foresti, P. A. Vigato, *Inorg. Chim. Acta* 2003, **353**, 292.
3. L. M. Hancock and P. D. Beer, *Chem. Commun.*, 2011, DOI: 10.1039/C1CC11224D.
4. L. M. Hancock, L. C. Gilday, S. Carvalho, P. J. Costa, V. Félix, C. J. Serpell, N. L. Kilah and P. D. Beer, *Chem. – Eur. J.*, 2010, **16**, 13082.
5. For crystal structures of other [3]rotaxanes see: (a) P. R. Ashton, P. T. Glink, J. F. Stoddart, S. Menzer, P. A. Tasker, A. J. P. White and D. J. Williams, *Tetrahedron Lett.*, 1996, **37**, 6217; (b) A. G. Kolchinski, N. W. Alcock, R. A. Roesner and D. H. Busch, *Chem. Commun.*, 1998, 1437; (c) N. Watanabe, T. Yagi, N. Kihara, T. Takata, *Chem. Commun.*, 2002, 2720; (d) Y. Furusho, T. Oku, T. Hasegawa, A. Tsuboi, N. Kihara, T. Takata, *Chem. – Eur. J.*, 2003, **9**, 2895; (e) V. Aucagne, J. Berná, J. D. Crowley, S. M. Goldup, K. D. Hänni, D. A. Leigh, P. J. Lusby, V. E. Ronaldson, A. M. Z. Slawin, A. Viterisi and D. B. Walker, *J. Am. Chem. Soc.*, 2007, **129**, 11950.
6. J. Cosier and A. M. Glazer, *J. Appl. Cryst.*, 1986, **19**, 105.
7. CrystalClear (Version 2.0, 2009), Rigaku Americas, 9009 TX, USA 77381-5209.
8. L. Palatinus and G. Chapuis, *J. Appl. Cryst.*, 1997, **40**, 786.
9. P. W. Betteridge, J. R. Carruthers, R. I. Cooper, K. Prout and D. J. Watkin, J. *Appl. Cryst.*, 2003, **36**, 1487.
10. (a) A. Spek, *J. Appl. Crystallogr.*, 2003, **36**, 7; (b) P. van der Sluis and A. L. Spek, *Acta Cryst.*, 1990, **A46**, 194.
11. M. J. Hynes, *J. Chem. Soc. Dalton Trans.*, 1993, 311.